Imaging with Charge-Coupled Devices

D. F. Barbe*
Naval Research Laboratory, Washington, D.C.

The small size and low power requirements, along with the potential for building up large focal planes from charge-coupled devices and charge-injection devices, make these devices very useful for space applications. This paper discusses the state-of-the-art in visible and infrared imaging devices which make use of the charge-coupled concept. Self-scanned two-dimensional CCD and CID arrays for visible imaging are compared. The use of CCD's in the time-delay-and-integration mode in mechanically scanned applications is described. Finally, the use of CCD's and CID's in infrared focal-plane arrays are discussed.

I. Introduction

UNTIL about a decade ago electronic devices for the pickup of optical images were in the form of vacuum-type camera tubes which depended on the scanning electron beam for signal readout. In such tubes the target is usually in the form of a thin evaporated film of photoconductor or, in later designs, in the form of a silicon wafer with an array of reverse-biased P-N junctions scanned by the beam. During the 1960's the availability of thin-film transistor technology was a stimulus to the development of soild-state arrays whose individual photoconductor elements were sensed via *X-Y* (horizontal and vertical) conductors connected to these elements and which are activated sequentially by voltages obtained from thin-film shift registers along the edges of the array.[1] At about the same time, other workers[2] demonstrated that optical images could be converted to electrical signals using a silicon wafer containing an array of phototransistors. Figure 1 shows a typical image produced from the output signals of such devices. Although such images were severely limited by response nonuniformities and other forms of spatial noise associated with the *X-Y* readout techniques, the work in the 1960's provided a fundamental understanding of the problems associated with such "self-scanned" solid-state camera devices.

Early in 1970 the simple but extremely powerful charge-coupled device (CCD) concept was introduced.[3] Basically, a charge-coupled device (CCD) is a metal-oxide-semiconductor (MOS) structure which can collect and store minority-carrier charge packets in localized potential wells at the $Si\text{-}SiO_2$ interface. Scene information is entered into the device via the controlled movement of potential wells. The charge packets then are detected at the output via capacitive coupling. Thus, the charge-coupled device permits charges collected at individual elements to be transferred in a linear fashion from element to element to the edge of the array where they can be read out as a time-varying signal. This technique provides several very important advantages. To a large degree it avoids the fixed pattern distrubances which are difficult to eliminate in *X-Y* scanned arrays. Also, the need for a transistor or other active element to be connected to each of the *X-Y* conductors of the earlier devices is avoided since only a few drivers are needed to accomplish the charge-transfer process. In addition, because of the lower capacitance across the input of the readout amplifier, considerably higher signal-to-noise ratios are obtainable. Aside from these advantages, the basic simplicity of the charge-coupled device concept, together with the availability of the well-developed MOS technology for use in fabricating CCD's, are responsible for the substantial advances which have been made in solid-state imaging during the last five years.

There are two types of charge-coupled device, surface-channel and buried-channel. In a surface-channel device, charge packets are stored and transferred at the interface between the silicon and the silicon dioxide. The position in the silicon where charge packets reside can be moved away from the silicon-silicon dioxide interface by doping the surface region of the P-type silicon substrate with N-type dopant. When the resulting P-N junction is reverse biased, the potential minimum is moved from the surface, where it was for a surface-channel device, into the bulk of the silicon. Since the charge packets in a buried-channel device do not contact the surface, effects of interface states are eliminated, and no bias charge is required. The buried-channel device has made ultralow-noise CCD's possible.

II. Visible Imaging

A. Two-Dimensional Self-Scanned Arrays

The arrays to be considered here are 1) the frame-transfer CCD, 2) the interline-transfer CCD, and 3) the charge-injection device. Figure 2 illustrates the general organizational features of the frame transfer CCD, the interline transfer CCD and CID chips. In the following analysis standard TV rates are assumed, i.e., 1/30 sec frame time and two vertically interlaced fields per frame.

In the frame-transfer structure, the top half of the chip is photosensitive. If a frame rate of 30 frames per second is assumed, then field A is formed by collecting photoelectrons under the ϕ-1 electrodes for 1/60 sec. This charge configuration is shifted into the shielded storage register in a time which is short compared with the integration time. Field A then is read out a line at a time while field B is being formed by collecting photoelectrons under the ϕ-2 electrodes.

In the interline-transfer structure, the shielded vertical readout registers are interdigitated with the photosensitive

Fig. 1 Imagery produced by a 256×256 element phototransistor array.

Received Sept. 13, 1976; presented as Paper 76-978 at the AIAA Systems Design Driven by Sensors Conference, Pasadena, Calif., Oct. 18-20, 1976; revision received Dec. 16, 1976.
Index category: Earth Satellite Systems, Unmanned.
*Head, Microelectronics Branch.

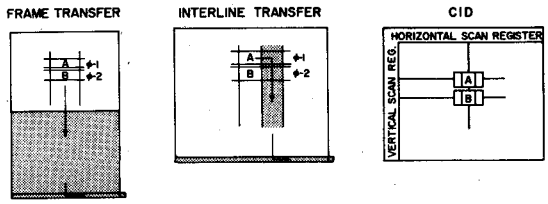

Fig. 2 Schematic diagrams showing the CCD frame-transfer, CCD interline-transfer, and CID array organizations.

column. Potential wells are formed in the photosensitive regions by applying voltages to the vertical polysilicon stripes. The horizontal polysilicon stripes are used to clock the vertical shielded register. Because the integrating cells and shift-out cells are separate, the effective integration time for both fields A and B is 1/30 sec. The operation is as follows. After collecting photoelectrons in field A for 1/30 sec, the charge configuration is shifted into the shielded registers and down, a line at a time, into the horizontal output register. When field A has been read out completely (1/60 sec), field B is shifted into the shielded registers and out. Note that the effective *integration* time for the interline-transfer structure is twice that of the frame-transfer structure because the integration in the interline transfer structure is performed in sites separate from the transport registers.

The integration process in a CID is the same as that in a CCD; i.e., charge is collected in potential wells. The readout of a CID is quite different from the CCD in that the CID is *X-Y* addressed. Intracell charge transfer occurs during readout; however, there is no intercell charge transfer in a CID. The integration time in a CID is 1/30 sec even though the field time is 1/60 sec. Field B is formed while field A is being read out and vice versa. The CID can be read out in two ways. 1) A given site (say the *i*th row-connected electrode and the *j*th column-connected electrode) can be read out by pulsing both the *i*th row-connected electrode and the *j*th column-connected electrode to ground. This collapses the potential well for that cell-site and the charge is injected into the substrate where it is detected as a current pulse. Charge in potential wells under other *i*th row-connected electrodes transfers to potential wells under column-connected electrodes, and charge in potential wells under other *j*th row-connected electrodes transfers to potential wells under column-connected electrodes, and charge in potential wells under other *j*th column-connected electrodes transfers to potential wells under *i*th row-connected electrodes. An array is read out by sequentially pulsing row-connected electrodes and column-connected electrodes to ground until all sites have been read out. 2) An alternate readout scheme involves a) the resetting of an electrode, b) the transfer of charge under it, and c) the sensing of the change of voltage on that line.

Figure 3 shows low-light-level imagery produced by a buried-channel 244×190 element CCD in 1974.[4] In this experiment a 100% contrast bar chart was imaged with a 244×190 buried-channel CCD at 0°C. In this experimental setup, the highest frequency bars are at half the Nyquist frequency. The CCD was operated at 30 frames per second, and the exposure time for the photographic film was 0.1 sec. Figure 3 shows the imagery as the target illumination was reduced. The signal was reduced from 2×10^5 electrons per pixel per frame in the highlights to 25 electrons per pixel per frame. Since the saturation level was 3×10^5 electrons, the dynamic range is 1.2×10^4 or 82 dB. A comparison of this imagery with that produced by solid-state arrays of the late 1960's shows the tremendous progress which has been made during the past five years. Figures 4 and 5 show imagery from large-area CCD arrays produced in 1975. The imagery shown in Fig. 4 was produced by a 488×380 array, and the imagery shown in Fig. 5 was produced by a 400×400 array.

An *X-Y* addressed device known as the charge-injection device (CID) also matured rapidly during the 1970's.[5] The

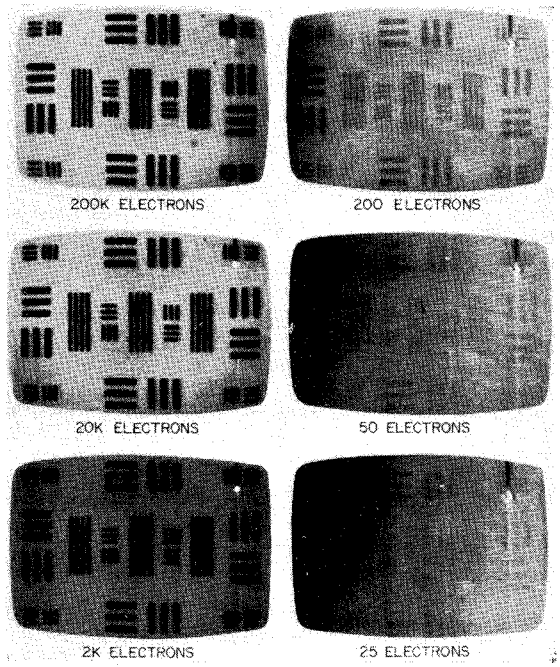

Fig. 3 Bar-chart imagery produced by a 244×190 element buried-channel interline-transfer array. The array temperature was 0°C, and the photographic exposure time was 0.1 sec. The number of electrons given in each photograph is the number of electrons per pixel per frame in the highlight regions.

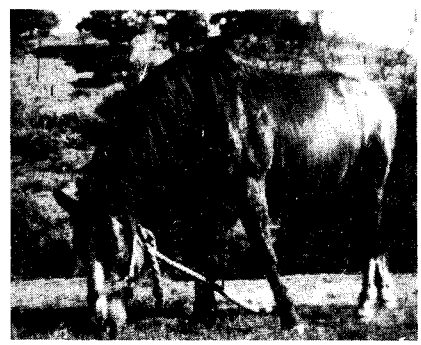

Fig. 4 Imagery produced by a buried-channel interline-transfer CCD 488×380 element array.

Fig. 5 Imagery produced by a buried-channel full-frame CCD 400×400 element array.

sensor cell for this device is composed of two coupled MOS capacitors. The CID uses intracell charge coupling, but not intercell charge coupling, during the readout process. Figure 6 shows an example of imagery from a 244×188 CID produced in 1975.

B. Serial-Parallel Scanned Arrays

In certain applications, it is important to view the object plane from a platform which has linear motion relative to the object plane. In such circumstances, the object/sensor motion

Fig. 6 Imagery produced by a 244 × 188 CID array.

may be used to generate one dimension of the image field. Typical examples of this type of image generation include strip and panoramic modes of aerial reconnaissance. This mode of image generation is commonly called the "push-broom" mode. Operating in the "pushbroom mode," as the sensor array moves across the scene due to the relative motion, the scene is synthesized into a series of strips. If a linear array is used, there is a tradeoff between signal-to-noise ratio and resolution in the along-track direction. The use of CCD's in the TDI mode has allowed the "pushbroom" concept to be extended to provide additional sensitivity (signal) without sacrificing resolution.

When the sensor and the scene to be viewed have a constant relative velocity, a linear array of sensor elements can be used for imaging. The minimum geometrically resolvable dimension in the along-track direction in the object plane d_{geom} is determined by the speed of the sensor projected onto the object plane via the optical system V_0 and the integration time of the sensor T, i.e.,

$$d_{geom} = V_0 T \tag{1}$$

where d_{geom} is the along-track distance covered by a sensor element projected onto the object plane in an integration time. Using the magnification relation, the speed of a point in the object plane projected onto the image plane V_i is

$$V_i = (f/r)\ V_0 \tag{2}$$

where

f = focal length of the optical system
r = object plane to image plane distance
V_0 = speed of a point in the image plane projected onto the object plane.

The output signal is proportional to the input irradiance H and the integration time, i.e.,

$$S \propto HT \tag{3}$$

Therefore, the product of the geometrical resolution and the signal out of the array is independent of T. This represents a basic tradeoff for the pushbroom mode; i.e., T can be reduced to decrease d_{geom}, but S also decreases.

If the image plane were composed of a number (M) of elements contiguous in the x direction to form an array of columns, if the columns were electrically delayed in the x direction at the same speed V_i as the scene is scanned across the image plane, and if the outputs from all elements in a given column were added, then the output signal would be M times larger than that from a single line array of equal elemental dimensions. This situation is called the time delay and integration mode. Other names are delay-and-add and image-motion compensation modes. The basic result is that the signal in Eq. (3) is increased by the factor M whereas geometrical resoltuion in Eq. (1) is unchanged. Thus, the new equations analogous to Eqs. (1) and (3) are

$$d_{geom} = V_0 T \tag{4}$$

and

$$S \propto HMT \tag{5}$$

A major advantage of the TDI mode is that the exposure time is increased by the factor M without affecting the geometrical resolution. This improves the low-light-level capability without affecting the resolution or data rate. The natural TDI CCD chip organization is basically a parallel-serial design. The parallel imaging columns are composed of M delay-and-add stages (CCD stages). These N columns are multiplexed into an N-stage CCD serial shift register for readout. There is no need for separate frame or line storage with this mode of operation; i.e., all of the columns are optically active. Only the horizontal output register is shielded from light.

For low-light levels, the TDI imager would operate in the noise limited regions; i.e., the minimum resolvable dimension in the along-track direction is given by

$$d_{min} = K\left[\frac{CSAMHT/e}{(SAMHT/e = MN_1^2 + N_2^2)^{1/2}}\right]^{-1} \times d_{geom} \tag{6}$$

where

C = scene constrast
S = responsivity in mA/W
A = optically active area of sensor element
M = number of TDI stages
T = integration time
H = irradiance on the image plane
e = electronic charge
N_1 = noise (in number of electrons) introduced at each TDI stage
N_2 = noise (in number of electrons) introduced by the output amplifier
K = the required signal-to-noise ratio, which depends on the type of detail to be resolved e.g., bar patterns, isolated squares, etc.

There are three cases to be examined with regard to the functional dependence of d_{min} on M: 1) if photon noise dominates, then d_{min} is proportional to $M^{-1/2}$; 2) if N_1 dominates, the d_{min} is proportional to $M^{-1/2}$; and 3) if N_2 dominates, then d_{min} is proportional to M^{-1}. TDI arrays having $M = 128$ have exhibited the geometrical resolution at an exposure of 1.4×10^{-6} J/m^2. This exposure results in the collection of less than two electrons per TDI stage.[6]

If the average speed of the charge packets is not exactly equal to the speed of the motion of the scene across the image plane, then the response will be degraded.[7] If the difference between the average speed of the charge packets $\bar{V}$ and the speed of the scene on the image plane V_i is ΔV, then after M TDI stages the charge packets will be displaced from where they should be if the synchronism were perfect, by the distance $MP(\Delta V/V)$. In effect the array sees a traveling wave instead of a fixed Fourier component representing each spatial frequency. The MTF degradation due to this effect can be determined by noting the equivalance between 1) an infinitesimal aperture sampling a traveling wave with relative speed ΔV for a time MP/V and 2) an aperture of width $MP(\Delta V/V)$ sampling a stationary wave. Therefore the form of this MTF is

$$(MTF)_{\Delta V} = \frac{\sin[(\pi/2)(f/f_n)M(\Delta V/V)]}{(\pi/2)(f/f_n)M(\Delta V/V)} \tag{7}$$

For $M(\Delta V/V) = 2$, the MTF is 0.64 at $f/f_n = 1/2$ and zero at $f/f_n = 1$. Further MTF degradation due to higher $M(\Delta V/V)$ would be intolerable. This is an important design criterion for TDI CCD arrays. If it is assumed that a practical value of $\Delta V/V$ is 1%, then using the criterion that $M(\Delta V/V) \leq 2$,

gives $M \leq 200$. Therefore for $\Delta V/V \simeq 1\%$, more than 200 delay-and-add stages is impractical. *The inequality* $M(\Delta V/V) \leq 2$ *is the primary criterion used to choose the number of TDI stages.*

III. Infrared Imaging

A. Focal-Plane Arrays

There are several devices which use the charge-coupled concept which are potentially useful for ir imaging applications. These devices are InSb CID, accumulation-mode CCD, and the extrinsic silicon photoconductor CCD. The operation of these devices will now be discussed.

1. InSb CID

The principle of operation of a InSb CID is the same as that of a silicon CID. The InSb CID uses chemically vapor deposited silicon oxynitride as the insulator. Interface state densitites of less than 10^{11} cm^{-2} have been achieved. Storage times of 100 msec at 77K have been reported (with no ir excitation). Responsivity and noise measurements have been made for 1-msec integration times on 16×24 element arrays. The results show that background-limited performance can be achieved for background levels down to 5×10^{12} photons/sec-cm^2 at an operating temperature of 77K.[8]

2. Accumulation Mode CCD

If an MIS structure is cooled to temperatures below impurity freezout, and if the gate-to-substrate bias is of the polarity to attract majority carriers to the insulator-semiconductor interface, then this element can be used as the basic element of an accumulation mode CCD (AMCCD) or accumulation mode CID (AMCID).[9] If the position of the doping level in the bandgap is ΔE with respect to the band edge, then photons of wavelength $\lambda = hc/\Delta E$ will be absorbed and will generate a majority carrier. If the doping density is large, the doping level will broaden into an impurity band in which case photon absorption will occur over a band of wavelengths with the absorption cutoff at $\lambda_c = hc/\Delta E$. Certain dopants in silicon have energy levels which correspond to ir wavelengths of interest; e.g., the cutoff wavelengths for Ga- and In-doped Si occur at about 18μ and 8μ, respectively. In this way the advantages of the well-developed silicon technology can be used for ir imaging. The disadvantage is the low temperatures required.

Figure 7 shows the energy bands for the basic MIS cell of an AMCCD below freezout. The energy bands have a linear dependence on distance into the silicon because of the absence of space charge. A 64-cell *n*-channel AMCCD has been fabricated on a 10^{15} cm^{-3} phosphorous-doped substrate. The transfer inefficiency was 10^{-1} at 25 kHz and 4.2K.

3. Extrinsic Silicon CCCD

The extrinsic silicon ir CCD uses the extrinsic silicon substrate (In or Ga doped) for detection and a CCD fabricated in an *n*-type epitaxial layer for readout.[10] The basic cell is shown in Fig. 8. The temperature must be low enough so that the dopant sites are neutral. A positive bias is applied to the P$^+$ layer on the backside of the substrate with respect to the frontside P$^+$ regions. The screen gate and storage gate are biased so that the photoconductive currents in the detector regions are integrated in the CCD storage sites. Charge is read out of the storage sites by pulsing the transfer gates to allow the charge flow into the CCD. The major advantage of this approach is that it uses silicon. Disadvantages are crosstalk and the operating temperature. The crosstalk problem arises because the absorption coefficient in extrinsic silicon detector elements is low; thus, thick substrates (10-20 mils) are required for sufficient sensitivity. However, crosstalk increases with increasing substrate thickness. The low temperature is required because the extrinsic dopant sites in the detector region must be neutral. This requires, for example, 30K for Ga-doped silicon and 60K for In-doped silicon.

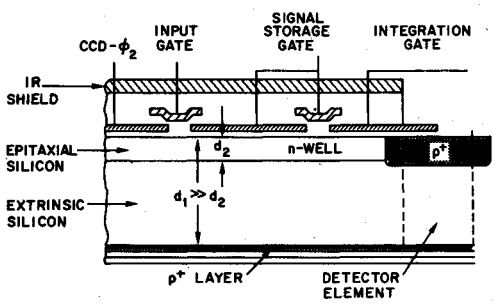

Fig. 8 The basic extrinsic silicon photoconductor cell.

B. Operational Modes

1. Staring Mode

In the staring mode the array integrates the full field of view for a period of time (1/60 sec for two-field TV compatible format) after which the field is read out while a second field is being integrated. The staring mode of operation is not suited for low-contrast, high-background thermal imaging because of the severe limits on the tolerable nonuniformity of response from element to element imposed by the combination of low contrast and high background. To illustrate this point, consider an array of ir elements operated in the staring mode. Assume that the mean responsivity of the elements is R and the deviation of the response of the ith element from the mean is ΔR_i. Let Q_b denote the photon background flux and C denote the contrast. After integrating for t_{integ} sec, the number of carriers in the ith CCD element is

$$N_i = (R + \Delta R_i) Q_b (1 + C) t_{\text{integ}}$$

$$= \underset{\text{(a)}}{R Q_b t_{\text{integ}}} + \underset{\text{(b)}}{R Q_b C t_{\text{integ}}} + \underset{\text{(c)}}{\Delta R_i Q_b t_{\text{integ}}} \qquad (8)$$

$$+ \text{negligible term}$$

Term (a) is a constant number of carriers in each cell and has no effect other than using dynamic range. Term (b) is the desired signal. Term (c) is the element-to-element variation in the number of carriers collected due to spatial nonuniformities of response. When the standard deviation of the distribution of terms (c) over the array is larger than (b), the signal will not be detectable. For example, in the 3-5μ range with a 290K background, the contrast is 4%/K. Thus, for a minimum resolvable temperature (MRT) of 0.2K the maximum nonuniformity tolerable is 0.8%. This imposes severe constraints on material homogeniety and photolithographic tolerances.[11] Since the nonuniformity in response is a fixed distribution over the array, its signature can be measured and stored in a memory. An element-by-element subtraction of the responsivity signature from the response to an actual ir scene can be used to reduce the MRT. The degree of improvement in the MRT depends on the accuracy of the signal processing (number of digital bits), and the signal processing may be expensive.

A second problem of staring mode operation in high-background ir imaging is that the high-background-flux densities may limit the integration to short times thereby

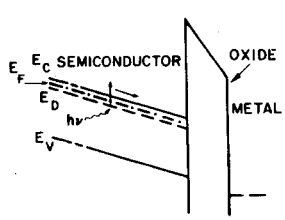

Fig. 7 Energy-band diagram for an accumulation mode CCD.

limiting the signal-to-noise ratio to low values. For example, full-well CCD carrier densities are typically less than 10^{12} cm^{-2}. The background flux density for $\lambda_c = 5\mu$ is approximately 10^{16} cm^{-2} sec^{-1}. Therefore, the maximum integration time which could be used is 100μsec.

2. *Parallel-Scanned Mode*

The parallel-scanned mode uses a linear array of sensor elements with rotating optics providing parallel scanning of the scene across the array. The sensors are usually photovoltaic HgCdTe of PbSnTe. CCD's with multiple inputs can be used to multiplex these arrays. The multiplexer implementation is shown in Fig. 9. Once per line time, the CCD, via the capacitively coupled input circuits, samples the detector output voltages, obtains charge in each CCD cell proportional to the corresponding detector output voltage, and shifts this charge configuration out. The object of this approach is to perform the multiplexing within the dewar with the least amount of power dissipation. In this way, the number of leads from the dewar to the outside world will be minimized and the heat load will be minimized. There are two problems associated with this approach: crosstalk between channels and the CCD output due to transfer inefficiency, and the low-noise injection of charge packets into the CCD which are proportional in charge to the voltage at the output of the detectors.[12] The crosstalk problem is solved largely by injecting into alternate CCD cells instead of injecting into each CCD cell. The larger problem is to introduce charge into the CCD in response to low-level voltages. Surface-channel CCD's would be surface-state noise limited; however, buried-channel CCD's with correlated double sampled output would be input noise limited. For an input capacitance of 0.2pF, the number of noise electrons due to input noise, $(kTC_{in})^{1/2}$, is 180 electrons. The corresponding noise voltage is $(kT/C_{in})^{1/2}$ which is 145μV. Since the input to the CCD is a voltage, it is the input noise voltage which must be minimized. This requires that C_{in} should be large.

3. *Serial-Scanned Mode*

The serial-scan mode utilizes one sensor element (or a few) to raster scan a field. The raster scan is achieved by optical scanning techniques.[13] The advantage as compared with parallel scan is better uniformity whereas the disadvantage is less sensitivity. A major advance was made when CCD delay-and-add- techniques were applied to the serial-scanned mode. This was called the discoid implementation. Today, time delay and integration (TDI) techniques are implied in the term serial scan. The feasibility of this approach was proven using an array of InSb detectors and a buried-channel CCD as shown in Fig. 10. TDI was achieved by making a 1:1 interconnection between each detector element and the corresponding CCD element via the appropriate low-noise input circuits. The charge injected into a CCD cell at a given point is proportional to the detector output voltage. The transfer of a charge packet along the CCD is synchronous with the velocity V_Q of the corresponding point in the image plane along the detector column. Thus, the effective signal is M times larger than the single-element signal, where M is the

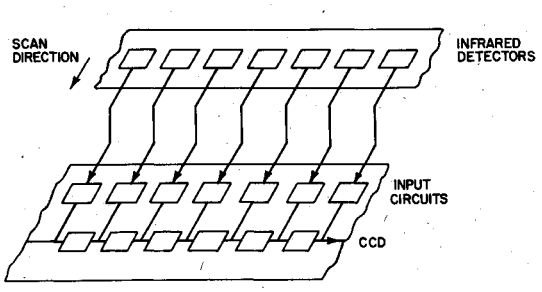

Fig. 9 Diagram showing the use of a parallel-in serial-out CCD for multiplexing a parallel-scanned detector array.

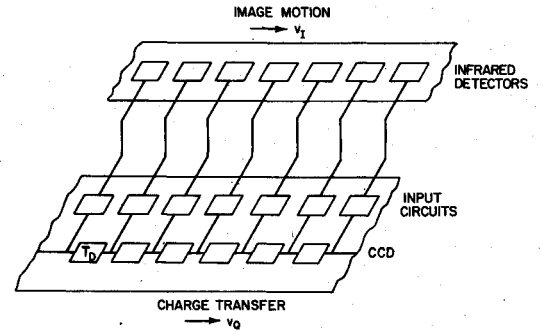

Fig. 10 Diagram showing the use of a parallel-in serial-out CCD to perform time-delay-and-integration on a serial-scanned detector array.

number of detectors in the column. Since the nosie is proportional to $M^{1/2}$, the signal-to-noise improvement over the single detector case is $M^{1/2}$. For an N-column by M-element image plane, the number of interconnections between the detector array and the CCD array is M times N. Reliable fabrication of this large number of interconnections is a major concern for this hybrid approach. The implementation of this mode with the monolithic extrinsic silicon approach or the AMCCD would eliminate the interconnection problem.

4. *Serial-Parallel Scanning Mode*

The serial-parallel scanning mode incorporates the advantages of the serial and parallel scanning, i.e., uniformity and sensitivity. Serial-parallel scanning incorporates parallel optical scanning and serial TDI. A serial-parallel scanned focal-plane array requires a two-dimensional array of detector elements. The number of detector elements perpendicular to the scan direction determines the number of lines which can be displayed. The number of elements parallel to the scan direction is the number of stages of TDI.

Monolithic focal-plane arrays can be fabricated using the AMCCD or extrinsic-silicon approaches; however, both of these arrays require very low temperatures (<77K). A serial-parallel scanned focal-plane array operating in the 3-5 μ range and operated at 77K can be fabricated using small InSb CID arrays. As an example this focal-plane array concept will be discussed in detail. The InSb CID module is a monolithic chip composed of 24 elements perpendicular to the parallel scan direction and 16 elements in the direction of parallel scan. A focal plane might, for example, be composed of seven of these chips positioned in such a way that they are optically contiguous. Each InSb CID would be read out by digital shift registers fabricated on silicon chips. Fabrication of the shift registers on the InSb CIB chips, of course, would reduce the number of wire bonds. This has not yet been done in InSb, although it now appears to be feasible. Each CID module would be read out through a single high-performance am-

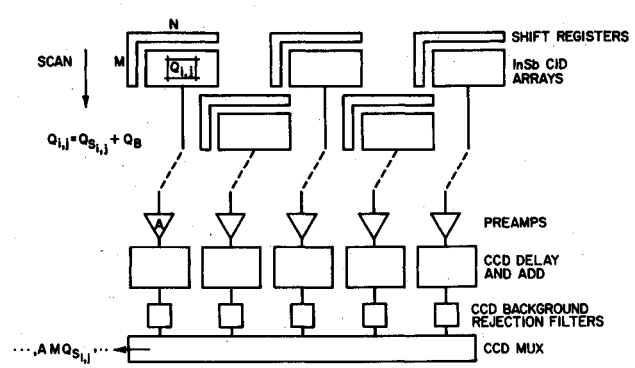

Fig. 11 Schematic diagram showing a focal-plane array using InSb CID detector arrays and silicon CCD arrays for time-delay-and-integration.

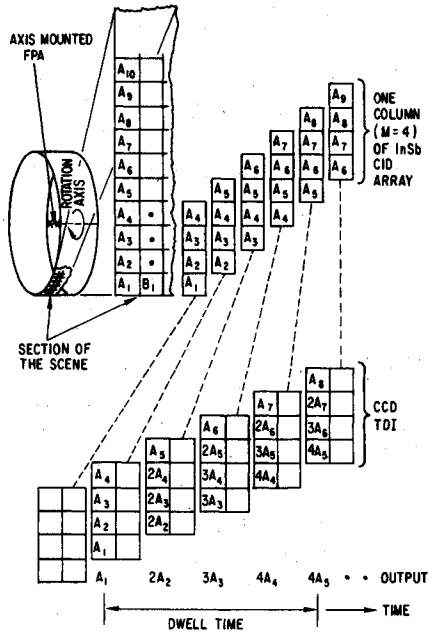

Fig. 12 Example of a serial-parallel scanned InSb CID focal-plane array operating in the search mode. Only four TDI elements and one channel are shown for simplicity.

plifier into a silicon CCD chip which would perform the TDI operation. High-pass CCD transversal filters could be used for background rejection, and a CCD multiplexer could be used to format the data for display. Figure 11 shows the complete focal plane.

If such a focal plane were mounted at the focus of a telescope, the telescope could be rotated to provide the parallel scan for an ir search set. Figure 12 illustrates the operation of the series-parallel mode. Only one channel having four delay-and-add elements is shown for simplicity. Note that for each CID column having M elements, two columns of M elements each are required in the silicon chip to provide the delay-and-add operation. As shown in Fig. 12, when the parallel scan moves one picture element, the data stored in the silicon shift registers is moved one element so that the charge from picture element A_i adds to that from picture element A_i from the previous CID readout. After an initial transient, the output, from the silicon chip is MA_i ($M=4$) for the example of Fig. 12.

In order to show the value of serial-parallel scanned focal-plane arrays, consider the detection range (R) of an ir search set. Assume that the imagery is noise limited and that the target subtends one sensor element or less and that the sensor noise is dominant. Then the signal-to-noise ratio (S/N) is proportional to R^{-2}. If TDI is performed on M sensor elements, then S/N is also proportional to $M^{1/2}$, i.e.

$$S/N \propto R^{-2} \propto M^{1/2} \tag{9}$$

thus

$$R \propto M^{1/2} \tag{10}$$

For example, using 16 TDI elements ($M=16$) would give an increase in range by a factor of 2 over the single sensor element case ($M=1$).

IV. Summary

Charge-coupled devices and charge-injection are having a major impact on visible and infrared imaging. In visible imaging the major useful properties of the CCD are 1) low temporal and spatial noise and 2) high responsivity. Also, the ability of the CCD to perform the TDI function is extremely useful in low-light-level applications where mechanical scan is inherent. The ability of CCD's to perform signal processing (TDI, filtering, and multiplexing) on the focal plane makes them especially useful in ir imaging.

References

[1]Weimer, P. K., "Image Sensors for Solid State Cameras," *Advances in Electronics and Electron Physics*, Vol. 37, Academic Press, New York, 1975, pp. 181-262.

[2]Schuster, M. A. and Strull, G., "A Monolithic Mosaic of Photo Sensors for Solid State Imaging Applications," *IEEE Transactions on Electron Devices*, Vol. 13, 1966, p. 906.

[3]Boyle, W. S. and Smith, G. E., "Charge Coupled Semiconductor Devices," *Bell System Technical Journal*, Vol. 49, 1970, pp. 587-593.

[4]Steffe, W., Walsh, L., and Kim, C. K., "A High Performance 190×244 CCD Area Image Sensor Array," *Proceedings of CCD Applications Conference*, San Diego, Calif., 1975, pp. 101-108.

[5]Burke, H. K. and Michon, G. J., "CID Imaging: Operating Techniques and Performance Characteristics," *IEEE Transactions on Electron Devices*, Vol. 23, 1976, pp. 189-196.

[6]Hunt, J. and Sadowski, H., *Proceedings of CCD Applications Conference*, San Diego, Calif., 1975, pp. 181-187.

[7]Soule, H. V., *Electro-Optical Photography at Low Illumination Levels*, John Wiley and Sons, New York, 1960, pp. 332-333.

[8]Kim, J. C., "High Sensitivity InSb CID Devices," *IRIS Detector Specialty Group Meeting*, San Diego, Calif., March 1976.

[9]Nelson, R. D., "Accumulation Mode Charge-Coupled Devices," *Applied Physics Letters*, Vol. 25, 1974, pp. 568-570.

[10]Candell, L. M. and Beckett, P. J., "Trends in Next Generation Thermal Imaging Using Integrated Focal Planes," *Conference on Laser and Electrooptical Systems*, San Diego, Calif., May 1976.

[11]Barbe, D. F., "Imaging Devices Using the Charge Coupled Concept," *Proceedings of IEEE*, Vol. 63, 1975, pp. 38-67.

[12]Cheeck, T. F., Barton, J.B., Emmons, S.P., Schroeder, J.E., and Tasch, A.F. Jr., *Proceedings of CCD Applications Conference*, San Diego, Calif., 1973, pp. 127-139.

[13]Erb, D. M. and Nummedal, K., "Buried Channel CCD's for Infrared Application," *Proceedings of CCD Applications Conference*, San Diego, Calif., 1973, pp. 157-167.